Theoretical study of structure-dependent Coulomb blockade in carbon nanotubes

Y. Q. Feng,* R. Q. Zhang,† K. S. Chan, H. F. Cheung, and S. T. Lee
Center of Super-Diamond and Advanced Films (COSDAF) & Department of Physics and Materials Science, City University of Hong Kong, Kowloon, Hong Kong SAR, China

(Received 16 August 2001; revised manuscript received 4 March 2002; published 3 July 2002)

The *I-V* characteristics and tunneling effects of several carbon nanotubes are studied by electronic transport calculations with a semiclassical approach. The electrical currents are obtained by solving master equations connecting different charge states. The charging energies and electronic structures of the nanotubes are calculated by the *ab initio* density-functional theory. The results show that the Coulomb blockade is closely related to the structures of systems, and that the necessary condition for the Coulomb staircase to occur is that the cathode junction is narrower than that of the anode. The Coulomb staircase, evident at lower temperatures, could be suppressed by temperature elevation.

DOI: 10.1103/PhysRevB.66.045404 PACS number(s): 73.63.Fg

I. INTRODUCTION

Some additional types of electronic devices can be designed with intrinsic quantum effects of nanostructures, in which the single-electron-tunneling (SET) effect is one of the most interesting observable phenomena.[1] Because the SET only appears noticeably in very small quantum islands or dots,[1,2] nanoparticles, nanotubes, and nanowires become ideal candidates for constructing molecular electronic devices, or nanodevices. To enable electrical transport through them, external electrode, which provides electrons to and accepts electrons from the nanostructures, must be applied. Such systems have been achieved using a scanning tunneling microscope (STM) by locating a metallic tip above a quantum dot separated from a conducting substrate.[2–4] Nanodevices have also been realized by connecting a nanotube with two lithographic metallic electrodes,[5–7] or by mechanically manipulating nanotubes accurately using atomic force microscope.[8,9] With the advances of nanotechnology, huge quantity of studies on carbon nanotube based tunneling systems has arisen in recent years.[3–12]

The atomic and electronic structural studies of single-walled carbon nanotubes (SWNTs) by STM and scanning tunneling spectroscopy (STS) were first reported in 1998.[13,14] At low temperature, the electron transport in nanotubes is usually dominated by Coulomb blockade.[1,15–17] Once an electron is imported into the quantum dot, it inhibits other electrons from joining until it is exported out, due to their Coulomb interactions. This inhibition could be broken down upon applying a bias voltage between the two electrodes so as to overcome the charging energy. With the bias voltage increasing, this breakdown appears repeatedly, inducing a transport current increase in a steplike manner, which is called Coulomb staircase. If temperature rises, the Coulomb staircase could be covered up by thermal effects. However, if the quantum dot is so small that its charging energy is greater than the thermal energy, the Coulomb blockade may be observed even at room temperature.[4] Nanotube transistor with such a behavior has been reported by Dekker and co-workers.[5,8] It represents a remarkable progress towards practical quantum devices.

The Coulomb staircase has been described quantitatively by several theories. In a simple classical capacity theory,[16] the system of the island and the junctions is represented by an equivalent circuit of a parallel combination of the tunneling capacity and resistance. Based on the truth that the system has to evolve from a state of a higher energy to the one of a lower energy, the theory gives that current-voltage curve presents the step feature with a step width inversely proportional to the capacity. Although it is an excellent approximation for metal islands, it only takes into account the difference of electrostatic energy before and after the injection of an electron and ignores the separation of electronic states occupied by the introduced electrons. Therefore, there would be limitations for such a theory to describe the electrical transport of nanoparticles. Nevertheless, the capacity-represented electrostatic energy is still applicable to other theories.[18–20]

Sander, Stanton, and Chang[21] proposed a quantum-mechanical method that incorporates band structure with phonon scattering. The electronic states are calculated by tight-binding approach, and the scattering rates are determined by Fermi golden rule. The results form the input of the Boltzmann transport equation, from which the transport properties of the system are obtained. Green's-function method[1,22] is also effective in studying the conductance of a nanotube. In this case, the conductance is given by the Landauer formula, in which a transmission function was obtained using the Green's function. The couplings of a nanotube with electrodes are described by self-energy terms of the interactions.

Another theory invoked widely is the so-called orthodox theory[16] developed by Averin and Likharev.[1] It adopts a kinetic equation for the occupation distribution of the charging states of the dot, reflecting the balance of in-scattering and out-scattering flows of electrons. Solving this equation, one can obtain the stationary occupation probabilities of the states. Based on them and the forward and backward tunneling rates of junctions, the average current is obtained. This theory has been further detailed by Beenakker.[23] The approach allows one a straightforward understanding of the physics involved in the theoretical results. However, the systems of quantum dots used for demonstrating the theory are all hypothetic simple models. It is expected that this ap-

 ©2002 The American Physical Society

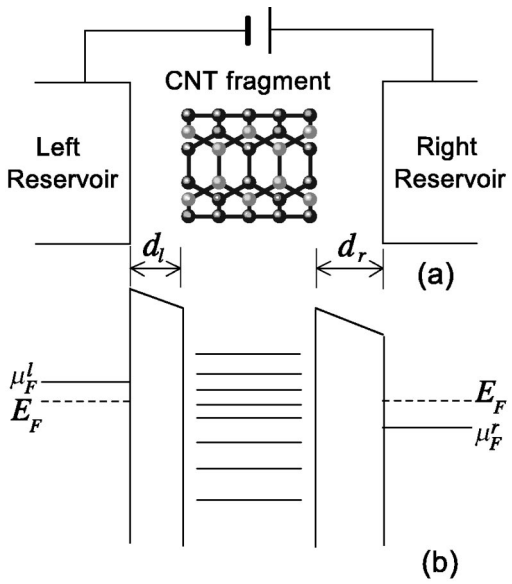

FIG. 1. (a) A schematic diagram of a nanotube fragment coupled with two electrodes through the tunnel junctions under a bias voltage. (b) A schematic diagram of the energy levels of a nanotube and the bias-induced energy band of the both metallic electrodes.

proach would find excellent application in the interpretation of experimental phenomena. In this work, we adopted this theory to investigate the quantum transport of carbon nanotubes. We aim to reveal the general trends about the electrical transport properties of the nanostructures.

II. THEORETICAL FORMALISM AND MODELS OF CARBON NANOTUBES

Figure 1(a) illustrates a carbon nanotube fragment which is weakly coupled with two electrodes through vacuum tunnel barriers. We selected gold as the STM tip and substrate and the transport of electrons can be described as the statistic results of subsequent tunneling events through the gold-nanotube-gold junctions.

The nanotube fragment is a confined quantum region, and therefore has a series of discrete single electronic levels ε_i, each of which is occupied by either one or zero electron. When extra electrons join the region, charge state is resulted. A joined electron increases the electrostatic energy by charging energy $E_c = e^2/2C$, where C is the capacitance of the dot to its surroundings. If N extra electrons fill the unoccupied levels, the increased total energy of the dot will be[23]

$$E_N = \sum_{i=1}^{N} \varepsilon_i + (Ne)^2/2C, \tag{1}$$

and the chemical potential will take

$$\mu_N = E_N - E_{N-1} = \varepsilon_N + (2N-1)E_c. \tag{2}$$

In the present work, the ε_i were obtained by calculations with a B3LYP method which uses Becke-type 3-parameter and Lee-Yang-Parr correlation functional of the density-functional theory and with a 3-21G basis set, carried out using a GAUSSIAN98 package.[24] Because C is not easy to obtain accurately, we calculated the charging energy E_c also by the B3LYP method.

We assume that the two gold electrodes acting as electron reservoirs possess continuum states in thermal equilibrium. Thus, the occupations of these states obey Fermi-Dirac distribution

$$f(E^{l,r} - \mu_F^{l,r}) = \{1 + \exp[(E^{l,r} - \mu_F^{l,r})/k_B T]\}^{-1}. \tag{3}$$

Here, the chemical potentials of both electrodes change with the applied bias voltage V_b,

$$\mu_F^l = E_F + (1-\eta)eV_b,$$

$$\mu_F^r = E_F - \eta eV_b, \tag{4}$$

in which E_F is the Fermi energy level without the bias, and η is a parameter related to the strength of coupling of the nanotube to the electrodes. We assumed V_b drops over both junctions according to their widths, $\eta = d_r/(d_l + d_r)$. The arising of electrical current at 0 K demands that the bias voltage is enough high so that the nanotube could provide at least one excited energy level locating between μ_F^l and μ_F^r. Such an energy level would facilitate the transport of electrons from the left to the right electrodes [see Fig. 1(b)].

Supposing that the tunneling processes from the nanotube to the electrodes or on the reverse direction be elastic, only the electrons satisfying energy relation $E^{l,r} = \mu_N$ could transfer between them.[23] The transition rates Γ of electrons through the tunnel barriers can be calculated by using Fermi golden rule,[16,23] For the tunneling at μ_N from the electrodes to the nanotube and for the reverse tunneling, we have

$$\Gamma_{l,r}^{+}(N) = (2\pi/\hbar)|T_N^{l,r}|^2 D_{l,r}(\mu_N) f(E^{l,r} - \mu_{l,r}),$$

$$\Gamma_{l,r}^{-}(N) = (2\pi/\hbar)|T_N^{l,r}|^2 D_{l,r}(\mu_N)[1 - f(E^{l,r} - \mu_{l,r})], \tag{5}$$

where $D(\mu_N)$ is the density of states of gold metal, and T_N is Hamiltonian matrix element for tunneling across the barriers. $|T_N|^2$ may be replaced, for simplification, by the transmission coefficient of a relevant triangular barrier with the WKB approximation[25]

$$|T_N|^2 = \exp\left(-\frac{4\sqrt{2m}}{3\hbar} d[\phi^{3/2} - (\phi - eV)^{3/2}] \right), \tag{6}$$

in which ϕ is the highest height of the barrier stridden over by an electron with energy μ_N, and V is the bias voltage drop over the junction. Thermal distribution is not applied to the nanotube fragment because its energy-level separation is much bigger than $k_B T$ even at room temperature.

Using Γ we may write the master equation[16,23] describing the time evolution of the probability $P(N)$ of extra N electrons in the nanotube

$$\frac{\partial P(N)}{\partial t} = \sum_{j=l,r} \{\Gamma_j^{+}(N-1)P(N-1) + \Gamma_j^{-}(N+1)P(N+1) - [\Gamma_j^{+}(N) + \Gamma_j^{-}(N)]P(N)\}. \tag{7}$$

Setting $\partial P(N)/\partial t=0$ and solving the linear equations, the stationary nonequilibrium probability $\tilde{P}(N)$ is obtained. Then, the average macroscopic current through the junctions is written as

$$I=e\sum_N \tilde{P}(N)[\Gamma_l^+(N)-\Gamma_l^-(N)]$$

$$=e\sum_N \tilde{P}(N)[\Gamma_r^-(N)-\Gamma_r^+(N)], \quad (8)$$

where the sum is over the number of all the possible extra electrons introduced to the nanotube. From the I-V curves solved in this way, some microscopic quantum effects in the transport of nanotubes would be expected.

In this work, we selected (3,3), (5,0), (5,5), and (6,0) carbon SWNT's as the quantum dots sandwiched between the electrodes for study. The (3,3) and (5,0) tubes have been theoretically predicted to be the smallest energetically favorable carbon nanotubes.[26] Their diameters are about 0.4 nm. As observed experimentally, the (3,3) or (5,0) tube may exist as the innermost tube of multiwalled nanotube (MWNT) with more than 10 shells, either deposited using mass-selected carbon ion beam deposition (the MWNT's are aligned in a *a*-C matrix on silicon substrate in this case) (Ref. 27) or produced by the arc discharge of graphite rods in a hydrogen atmosphere.[28] Such small carbon nanotubes were also found inside the one-dimensional channels of a single-crystal zeolite.[29] Although no free-standing (3,3) and (5,0) carbon nanotubes have been observed experimentally, a theoretical study on their electrical transport with respect to the tube and device structures based on first-principle calculations of electronic structures may provide insight to the basic characteristics of nanotube based quantum devices. We designed four models of the (3,3) nanotube with different lengths in order to reveal the transport property in relation to the dimensional parameter. A (5,5) tube was also considered in this work, as it is possibly the smallest free-standing SWNT found so far with a diameter of 0.7 nm.[30] In addition, a (6,0) tube was used for comparison with the (5,0) tube, since they are all zigzag-type tubes but with different diameters. The adopted nanotube models are shown in Fig. 2.

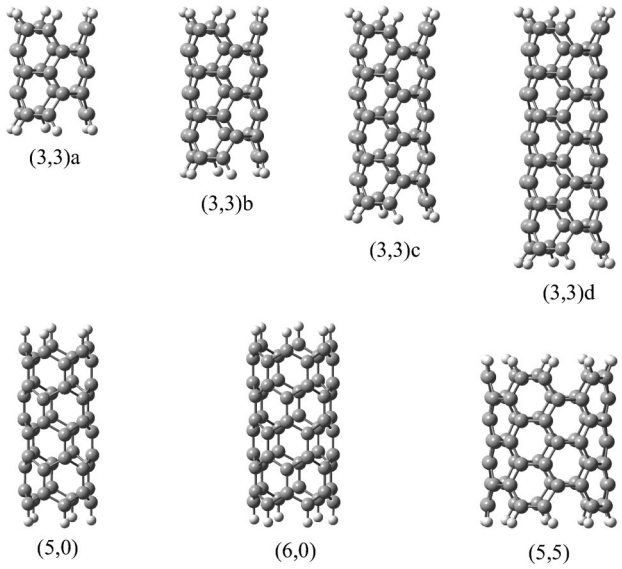

FIG. 2. The atomic structures of several nanotube models adopted in this work. On the both ends of tubes, the dangling bonds are saturated with hydrogen atoms.

III. RESULTS AND DISCUSSION

A. Charging energies

The charging energy is a key factor in determining the electrical transport of quantum nanostructures. The extra electrons entering a quantum dot would fill up empty energy levels possibly with some relaxation occurring. The charging energy can be obtained by the difference in an energy level before and after being occupied by an extra electron[31]

$$E_c=[\varepsilon_{\mathrm{HOMO}}(N)-\varepsilon_{\mathrm{LUMO}}(N-1)]/2, \quad N=1,2,..., \quad (9)$$

where $\varepsilon_{\mathrm{LUMO}}(N-1)$ and $\varepsilon_{\mathrm{HOMO}}(N)$ are, respectively, the lowest unoccupied level of the nanostructures with $N-1$ extra electrons and the highest occupied level of the nanostructures with N extra electrons. Using Eq. (9), we calculated the E_c of C_{60} for $N\approx 1,2,...,6$ from the data reported by Green *et al.*[32] As seen from the data listed in Table I, the calculated E_c are all around 1.50 eV. However, the E_c values obtained by fitting to experimental current-voltage results of adsorbed C_{60} by STS are just 0.35 or 0.20 eV.[33] The large difference may be mainly due to the fact that the system measured in experiment involves considerable interactions between C_{60} and the metallic electrodes. Direct calculations of charging energy for the nanotube-electrode interaction systems are difficult using *ab initio* theory. In order to include the electrode-nanostructure interaction in our calculations so that the calculated transport characteristics could be compared with experimental results, we scaled the E_c calculated using Eq. (9) by a factor of 0.15 (estimated by referencing to the C_{60} system). The scaled E_c are shown in Table I and will be used in the calculation of the I-V curves.

For the four (3,3) tubes in Fig. 2 marked with *a*, *b*, *c*, and *d* according to their differences in lengths, the calculated data of E_c as listed in Table I show clearly that the bigger the size of clusters the smaller the corresponding E_c, and vice versa. This is probably the main reason why our results are very different from the experimental charging energy (25 meV) by Cobden *et al.*, [34] where the nanotubes are 100–200 nm in length, much longer than the nanotubes we considered here. In addition, our calculations gave smaller E_c for the (5,5) tube clusters than that for the (3,3) with same length (*b* structure). This can also be explained with this size effect.

B. Basic characteristics and temperature effects

We selected the (5,0) carbon nanotube as a representative to study the transport characteristics of nanotubes. Its electronic energy-level spectrum is illustrated in the inset of Fig. 3. By applying a bias voltage, the chemical potentials μ_F^l and μ_F^r of the left and right electrodes move away from the Fermi level. When the bias voltage increases to a value that enables the electronic energy level of a tube entering the

TABLE I. The charging energy E_c of the nanotube models. The E_c of the model structures coupled with electrodes are obtained by scaling the E_c of the isolated model structures by a factor of 0.15. The E_c of C_{60} are also listed for comparison. They are calculated based on the data provided in Ref. 32. (Unit of energy: eV)

Nanotube	Atom number	Length (nm)	$\varepsilon_{\mathrm{LUMO}}(0)$	$\varepsilon_{\mathrm{HOMO}}(1)$	E_c (Isolated)	E_c (Coupled)
(3,3) *a*	30	0.49	−1.828	0.818	1.32	0.198
(3,3) *b*	42	0.74	−2.625	−0.223	1.20	0.180
(3,3) *c*	54	0.99	−2.330	−0.128	1.10	0.165
(3,3) *d*	66	1.24	−2.819	−0.927	0.95	0.142
(5,5)	70	0.74	−2.431	−0.451	0.99	0.148
(5,0)	50	0.64	−3.147	−1.417	0.86	0.129
(6,0)	60	0.64	−3.410	−0.936	1.24	0.186
Fullerene	Extra electron number N		$\varepsilon_{\mathrm{LUMO}}(N-1)$	$\varepsilon_{\mathrm{HOMO}}(N)$	E_c (Isolated)	E_c (Coupled)
C_{60}^{-}	1		−4.760	−1.770	1.50	0.225
C_{60}^{2-}	2		−1.770	1.285	1.53	0.230
C_{60}^{3-}	3		1.335	4.305	1.48	0.222
C_{60}^{4-}	4		4.305	7.310	1.50	0.225
C_{60}^{5-}	5		7.310	10.300	1.50	0.225
C_{60}^{6-}	6		10.300	13.240	1.47	0.220

range between μ_F^l and μ_F^r, the nanotube acts as a path for electron transport, leading to a sudden rise in the current. Figure 3 presents the *I-V* curves of this cluster at different temperatures. An obvious feature is the Coulomb staircase, especially at low temperatures. Some plateaus ranges present between two contiguous steps. The widths of these plateaus ΔV_N are determined by

$$(1-\eta)e\Delta V_1=\mu_1-E_F=\varepsilon_1-E_F+e^2/2C, \qquad (10a)$$

$$(1-\eta)e\Delta V_N=\mu_N-\mu_{N-1}=\varepsilon_N-\varepsilon_{N-1}+e^2/C,$$
$$N=2,3,\ldots. \qquad (10b)$$

Using this equation, one can obtain the capacity C if ΔV_N and energy spectra are determined. In addition, the effective

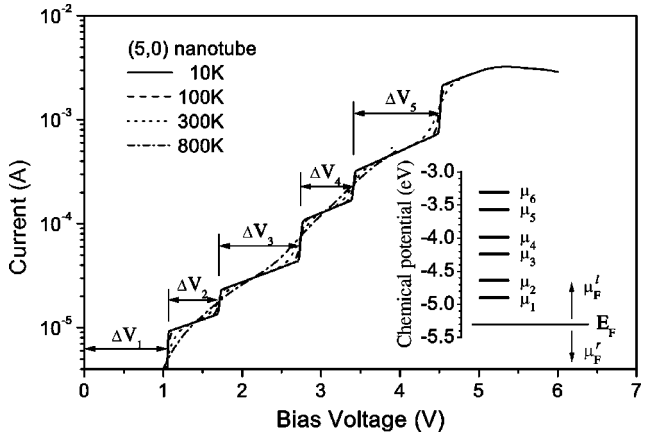

FIG. 3. The *I-V* characteristics of the (5,0) nanotube model at different temperatures, with the junction widths of $d_l=0.5$ and $d_r=0.8$ nm. The inset shows the chemical potentials of the tube above the Fermi energy level of electrodes without a bias. The trends of Fermi chemical potential change of the electrodes with the increased bias voltage are marked with arrows.

resistances of junctions may also be obtained from the step heights.[2] After several steps, the plateau feature stops and the current falls down. This will be further discussed in Sec. III E.

It is noted that single-electron energy levels of nanotubes are spin degenerate, each of which is occupied by two electrons with different spins. If extra electrons join, the energy levels are split off. For example, the $\mu_1=\varepsilon_1+E_c$ and $\mu_2=\varepsilon_2+3E_c$, in the inset of Fig. 3, corresponding to two steps at the both ends of ΔV_2 in the *I-V* curves, are split from a pair of degenerate levels ($\varepsilon_1=\varepsilon_2$) of the nanostructure before the extra electrons joining. Similarly, μ_3 and μ_4 are from $\varepsilon_3=\varepsilon_4$. Consequently, $\Delta V_2=\Delta V_4=e/C(1-\eta)$ can be obtained from Eq. (10). They are the smallest plateau widths. Such a feature of small, equal-width, alternatively appearing plateaus provides an important identity for tracing the spin-degenerate level evolution. In other words, the steps appear pair by pair with the increasing of bias voltage, corresponding to even and odd extra electrons consecutively joining the nanotube. It has been evidenced experimentally that there are alternative changes in conductance peak with gate voltage,[34] which also correspond to the accommodation changes from odd to even extra electrons in the nanotube. The spin related tunneling events presented in our work are similar to those observed in their experiments. Such a correlation between the spin interaction and the Coulomb blockade in nanotubes has also been demonstrated in other theoretical work. [20]

When temperature rises, the steps become less abrupt. This indicates that the Coulomb staircase can be suppressed by the thermal effects. If we replace the short nanotube fragment with a longer one (with smaller charging energy and energy level separation), the plateaus will be narrower and thus be easily smeared by the thermal effects. Therefore, it can be deduced that the Coulomb staircase will vanish at a lower temperature for the longer nanotube. Estimated by a

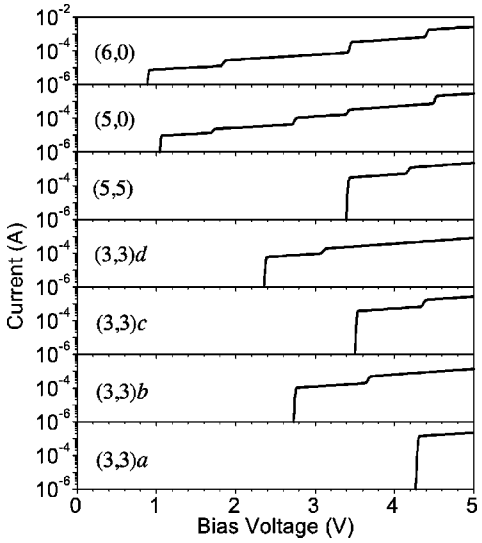

FIG. 4. The *I-V* characteristics of all nanotube models considered in this work at 10 K and with the junction widths of $d_l = 0.5$ and $d_r = 0.8$ nm.

proportional trend, the Coulomb staircase phenomenon for a step width of 0.1 V would not be observable over 30 K.

C. Effects of nanostructure

With the increasing of the bias the electrons keep blocked from entering the quantum dots until the first steps appear in the *I-V* curves. The forbidden ranges ΔV_1 provide the information about charging energies and band gaps of the nanotubes, as seen from Eq. (10a) for $N=1$. Figure 4 shows the *I-V* curves of the (3,3), (5,5), (5,0), and (6,0) nanotubes, in which current-blocked ranges (without current) are obviously seen. The widths of the ranges are very important for designing molecular devices.

Among the four (3,3) tube models, *c* can be obtained by extending a lattice period, respectively, at both ends of *a*, and so can *d* from *b*. Consequently, *a* and *c* show some related feature and the current-blocked range of the former is bigger than that of the latter. Similar features are shown between *b* and *d*. From the trends, one can expect the reduction of the energy gap of the tubes on increasing the dimension, where the gap V_g is related to ΔV_1 by $(1-\eta)e\Delta V_1 = V_g/2 + e^2/2C$. The (5,5) tube model has the same length as the $(3,3)b$ model but possesses a bigger diameter than it. The gap of the former should be narrower than that of the latter according to the report by Odom *et al.*[13] However, Fig. 4 gives a different result. We conjecture that the large gap of the (5,5) tube might be due to its short length and large number of the hydrogen atoms used for saturating its dangling bonds. In addition, the *I-V* curves of the (5,0) and (6,0) tube models are very different from others: they have much smaller noncurrent ranges, thus much narrower gaps. This suggests some metallic characters of the both tube models.

D. Contact effects

The coupling of nanotubes with electrodes can be incorporated in the simulation by considering the junction widths

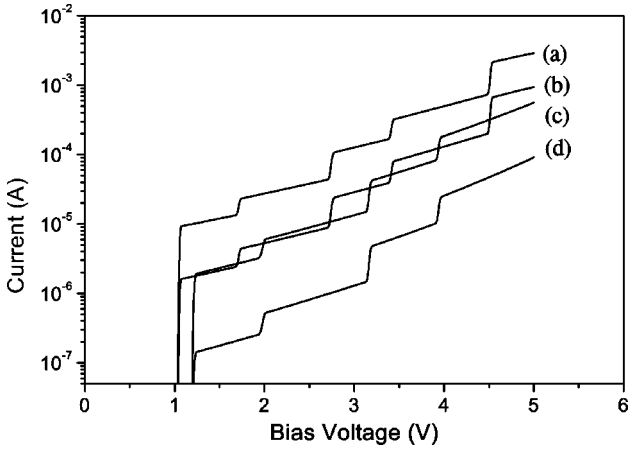

FIG. 5. The *I-V* characteristics of the (5,0) tube cluster at 10 K, with the junction widths of (a) $d_l = 0.5$, $d_r = 0.8$; (b) $d_l = 0.55$, $d_r = 0.88$; (c) $d_l = 0.44$, $d_r = 0.88$; and (d) $d_l = 0.5$, $d_r = 1.0$ nm.

in addition to the scaling of charging energies. The narrower the junctions are, the stronger the coupling is. Because the transmission coefficient is very sensitive to junction width as described in Eq. (6), the width ratio of both junctions is an important factor affecting the transport properties. Figure 5 presents the *I-V* curves for different junction width ratios. With the widths $d_{l,r}$ of the left and right junctions increased proportionally, although the positions of steps keep unchanged, the currents fall very sensitively within the same plateau range [curves $(a)-(b)$; $(c)-(d)$]. Keeping the d_l unchanged but increasing the d_r, one can find the ascent of the plateau widths and the descent of the current [(a) and (d)]. On the contrary, keeping the d_r unchanged but increasing the d_l, the current is hardly changed and only the plateau widths are increased [(b) and (c)]. Therefore, the current is approximately controlled by the right junction, which will be further discussed in the following section. In the plateau ranges, the currents, in fact, increase exponentially with the bias. This can be attributed to the fact that the transmission coefficient follows nearly an exponent relation to the product of width and bias voltage drop of junction, as deduced from Eq. (6).

E. General discussion

We found that the Coulomb staircase only takes place for the case of $d_l < d_r$. This means that the transmission coefficient of the left junction is bigger than that of the right one under a moderate bias. Therefore, the transport bottleneck is the right barrier. As soon as an electron tunnels out of the tube through the right junction, the tube is immediately replenished through the left junction. In other words, the tube always fills with electrons that can be offered to the right electrode. According to our calculation, $\tilde{P}(N_{\max})$ ($N_{\max}$ is the maximum possible electron quantity in the nanostructure for a given bias) is much bigger than those for other *N*. This means that all energy levels of the tube between μ_F^l and μ_F^r tend to be occupied completely. With the bias increasing, μ_F^l rises to be higher and μ_F^r falls to be lower. Once an energy level falls into the range between μ_F^l and μ_F^r, it is occupied

immediately, resulting in a new path in the tube for collecting (emitting) electrons out of (to) the reservoir and a rapid rise or an abrupt step of the current.

On the other hand, when $d_l > d_r$, the transmission coefficient of the left junction is smaller than that of the right, and the transport bottleneck is the left junction. Although a current can be produced in the system, the tube keeps unoccupied for all energy levels above E_F according to our calculation. This means that the appearance of the energy levels between μ_F^l and μ_F^r cannot enhance the transport capability of the tube. Therefore no Coulomb staircase appears for this case.

As to the special current dropping at the tail of the *I-V* curve in Fig. 3, a possible explanation is given below. When the bias is increased to a certain value, the left junction barrier is too high compared to its right-hand-side counterpart. The superiority of the left junction in the transmission coefficient because of $d_l < d_r$ is deteriorated by its barrier height increase. As a result, the transmission coefficient of the left junction becomes lower than that of the right junction, and the Coulomb staircase and the plateaus will not appear. Consequently, at most five electrons can be injected into the (5,0) tube model. It is worth mentioning that in transport calculations[35] only three electrons were found to be stored in C_{60} which is of the similar size as the (5,0) tube model we considered here, probably due to the same reason.

IV. SUMMARY

In the present work, we studied the electronic transport properties of several nanotubes sandwiched between two metallic electrodes by calculating their current-voltage characteristics. The currents are resulted from the tunneling effect between the nanotubes and the electrodes under a bias voltage, and are obtained by solving master equations connecting the different charge states of nanotubes. The charging energies and electronic structures are calculated by *ab initio* density-functional theory. The calculated *I-V* curves present the feature of staircase, indicating the Coulomb blockade. It only occurs at lower temperatures, and may be covered up by thermal effect at elevated temperatures. Our study on the effects of the nanotube structures and coupling to the electrodes on the Coulomb blockade indicates that the necessary condition of the Coulomb staircase occurring is that the cathode junction is narrower than the anode junction.

ACKNOWLEDGMENTS

This work was jointly supported by two grants from the Research Grant Council of the Hong Kong Special Administrative Region, China [Project No. 9040633/CityU, 1011/01P; and Project No. 8730016/CityU, 3/01C].

*On leave from Beijing Institute of Technology, Beijing 100081, China.

†Corresponding author, FAX: +852-2788-7830. Email address: aprqz@cityu.edu.hk

[1] D. V. Averin and K. K. Likharev, *Mesoscopic Phenomena in Solids*, edited by B. L. Altshuler, P. A. Lee, and R. A. Webb (Elsevier, Amsterdam, 1991).

[2] R. Wilkins, E. Ben-Jacob, and R. C. Jaklevic, Phys. Rev. Lett. **63**, 801 (1989).

[3] J. Hu, M. Ouyang, P. Yang, and C. M. Lieber, Nature (London) **399**, 48 (1999).

[4] M. Dorogi, J. Gomez, R. Osifchin, R. P. Andres, and R. Reifenberger, Phys. Rev. B **52**, 9071 (1995).

[5] S. J. Tans, A. R. M. Verschueren, and C. Dekker, Nature (London) **393**, 49 (1998).

[6] S. J. Tans, M. H. Devoret, R. J. A. Groeneveld, and C. Dekker, Nature (London) **394**, 761 (1998).

[7] D. C. Glattli, Nature (London) **393**, 516 (1998).

[8] H. W. Ch. Postma, T. Teepen, Zhen Yao, M. Grifoni, and C. Dekker, Science **293**, 76 (2001).

[9] H. W. Ch. Postama, M. Jonge, Zhen Yao, and C. Dekker, Phys. Rev. B **62**, R10 653 (2000).

[10] M. Bockrath, D. H. Cobden, Jia Lu, A. G. Rinzler, R. E. Smalley, L. Balents, and P. L. McEuen, Nature (London) **397**, 598 (1999).

[11] D. L. Klein, P. L. McEuen, J. E. B. Katari, R. Roth, and A. P. Alivisatos, Appl. Phys. Lett. **68**, 2574 (1996).

[12] J. Nygård, D. H. Cobden, M. Bockrath, P. L. McEuen, and P. E. Lindelof, Appl. Phys. A: Mater. Sci. Process. **A69**, 297 (1999).

[13] T. W. Odom, J. Huang, P. Kim, and C. M. Lieber, Nature (London) **391**, 62 (1998).

[14] J. Wildoer, L. Venema, A. Rinzler, R. Smalley, and C. Dekker, Nature (London) **391**, 59 (1998).

[15] J. Weis, R. J. Haug, K. v. Klitzing, and K. Ploog, Semicond. Sci. Technol. **9**, 1890 (1994).

[16] D. K. Ferry and S. M. Goodnick, *Transport in Nanostructures* (Cambridge University Press, Cambridge, U.K., 1997).

[17] H. W. Ch. Postma, M. Jonge, Zhen Yao, and C. Dekker, Phys. Rev. B **62**, R10 653 (2000).

[18] J. Weis, R. J. Haug, K. v. Klitzing, and K. Ploog, Phys. Rev. B **46**, 12 837 (1992).

[19] K. Jauregui, W. Häusler, D. Weinmann, and B. Kramer, Phys. Rev. B **53**, R1713 (1996).

[20] M. Mehrez, Hong Guo, Jian Wang, and C. Roland, Phys. Rev. B **63**, 245410 (2001).

[21] G. D. Sanders, C. J. Stanton, and Y. C. Chang, Phys. Rev. B **48**, 11 067 (1993).

[22] D. Orlikowski, H. Mehrez, J. Taylor, Hong Guo, Jian Wang, and C. Roland, Phys. Rev. B **63**, 155412 (2001).

[23] C. W. J. Beenakker, Phys. Rev. B **44**, 1646 (1991).

[24] M. J. Frisch, G. W. Trucks, H. B. Schlegel, G. E. Scuseria, M. A. Robb, J. R. Cheeseman, V. G. Zakrzewski, J. A. Montgomery, Jr., R. E. Stratmann, J. C. Burant, S. Dapprich, J. M. Millam, A. D. Daniels, K. N. Kudin, M. C. Strain, O. Farkas, J. Tomasi, V. Barone, M. Cossi, R. Cammi, B. Mennucci, C. Pomelli, C. Adamo, S. Clifford, J. Ochterski, G. A. Petersson, P. Y. Ayala, Q. Cui, K. Morokuma, D. K. Malick, A. D. Rabuck, K. Raghavachari, J. B. Foresman, J. Cioslowski, J. V. Ortiz, A. G. Baboul, B. B. Stefanov, G. Liu, A. Liashenko, P. Piskorz, I. Komaromi, R. Gomperts, R. L. Martin, D. J. Fox, T. Keith, M. A. Al-Laham, C. Y. Peng, A. Nanayakkara, M. Challacombe, P. M. W. Gill, B. Johnson, W. Chen, M. W. Wong, J. L. Andres, C. Gonzalez, M. Head-Gordon, E. S. Replogle, and J. A. Pople, GAUSSIAN98, Re-

vision A.9 (Gaussian, Inc., Pittsburgh PA, 1998).
[25] A. Selloni, P. Carnevali, E. Tosatti, and C. D. Chen, Phys. Rev. B **31**, 2602 (1985).
[26] S. Sawada and N. Hamada, Solid State Commun. **83**, 917 (1992).
[27] H. Y. Peng, N. Wang, Y. F. Zheng, Y. Lifshitz, J. Kulik, R. Q. Zhang, C. S. Lee, and S. T. Lee, Appl. Phys. Lett. **77**, 2831 (2000).
[28] L.-C. Qin, X. Zhao, K. Hirahara, Y. Miyamoto, Y. Ando, and S. Iijima, Nature (London) **408**, 50 (2000).
[29] N. Wang, Z. K. Tang, G. D. Li, and J. S. Chen, Nature (London) **408**, 50 (2000).
[30] P. M. Ajayan and S. Iijima, Nature (London) **358**, 23 (1992).
[31] H. van Houten, C. W. J. Beenakker, and A. A. M. Staring, in *Single Charge Tunneling*, edited by H. Grabert and M. H. Devoret (Plenum, New York, 1992).
[32] W. H. Green, S. M. Gorun, G. Fitzgerald, P. W. Fowler, A. Ceulemans, and B. C. Titeca, J. Phys. Chem. **100**, 14 892 (1996).
[33] D. Porath, Y. Levi, M. Tarabiah, and O. Millo, Phys. Rev. B **56**, 9829 (1997).
[34] D. H. Cobden, M. Bockrath, P. L. McEuen, A. G. Rinzler, and R. E. Smalley, Phys. Rev. Lett. **81**, 681 (1998).
[35] J. J. Palacios, A. J. Perez-Jimenez, E. Louis, and J. A. Verges, Nanotechnology **12**, 160 (2001).